Solutal Convection in Confined Geometries: Enhancement of Colloidal Transport

B. Selva, L. Daubersies, and J.-B. Salmon
Université Bordeaux, CNRS, Rhodia, LOF, UMR 5258, F-33680 Pessac, France
(Received 14 December 2011; published 9 May 2012)

We evidence experimentally and theoretically that natural convection driven by solutal density differences in a molecular binary mixture can boost the transport of colloids. We demonstrate that such buoyancy-driven flows have a negligible influence on the gradients that generate them, for moderate Rayleigh numbers in a confined geometry. These flows therefore do not *homogenize* the binary mixture but can disperse very efficiently large solutes. We illustrate the relevance of such effects thanks to several original experiments: drying of confined droplets, microfluidic evaporation, and interdiffusion in microfluidic flows.

DOI: 10.1103/PhysRevLett.108.198303 PACS numbers: 82.70.Dd, 47.55.P−, 47.61.Jd

Natural convection, i.e., flows induced by differences of density that generate buoyancy forces, has been the focus of intense research during the past 50 years, in a wide range of topics: physics of oceans, insulation of buildings, etc. [1] Density differences arise either from thermal or solutal gradients and lead to buoyancy-induced convection that can modify heat and mass transfers in a complex way [1]. For a thin liquid layer confined between two plates of length L separated by a distance h (Fig. 1), density gradients ($\delta\rho/L$) orthogonal to the gravity $\boldsymbol{g}$ *always* lead to a buoyancy-driven flow U, as there is no critical threshold for convection [1]. A scaling estimate for U can be obtained from a simple balance between buoyancy ($gh\delta\rho/L$) and viscous forces ($\eta U/h^2$) [2]. For solutal gradients within the fluid, $U \sim (\delta\phi/L)\rho' g h^3/\eta$, where the density is $\rho(\phi) = \rho_0 + \rho'\phi$, ϕ being the volume fraction of solute, and $\delta\phi/L$ the concentration gradient. The significance of this natural convection for the transport of the solute ϕ is governed by the ratio of convective to diffusive fluxes [2]:

$$\frac{Uh}{D} = \frac{\rho'\delta\phi g h^4}{\eta L D} = \mathrm{Ra}, \tag{1}$$

where D is the diffusion coefficient of the solute and we introduce the Rayleigh number Ra. Since $\mathrm{Ra} \sim h^4$, diffusion dominates the transport of solute in confined geometries [2], often leading to the erroneous conclusion that such buoyancy-driven flows are negligible.

In the present Letter, we first go beyond the above scaling estimate of U and demonstrate thanks to the lubrication approximation that diffusion still dominates the transport of ϕ, for $\mathrm{Ra} < \mathcal{O}(1)$ in a confined geometry ($h \ll L$). Yet, convection still persists up to the complete relaxation of the concentration gradients and has an impact on the transport of *less mobile* solutes such as dilute colloids dispersed in the fluid. Indeed, the significance of convection over diffusion is now estimated thanks to $Uh/D_c = \mathrm{Ra}D/D_c$ (D_c is the diffusion coefficient of the colloids), that can reach high values for $D_c \ll D$.

In the following, we first demonstrate this striking result and then report several experiments that generate weak transverse concentration gradients within binary mixtures, thus leading to *sustained* buoyancy-driven flows. In these confined geometries, concentration gradients arise either by the evaporation of the solvent (from confined droplets or from microchannels) or during transverse mixing between coflowing liquid streams in a microchannel. In these experiments, natural convection negligibly influences the solutal gradients that generate it but strongly enhances the transport of colloids dispersed in the fluid.

We first consider the case of a simple binary mixture in a confined geometry (Fig. 1), with constant interdiffusion coefficient D and viscosity η. Within the lubrication approximation and at a small Reynolds number, the volume-averaged velocity $\boldsymbol{u} = (u_x, u_z)$ follows [3,4]:

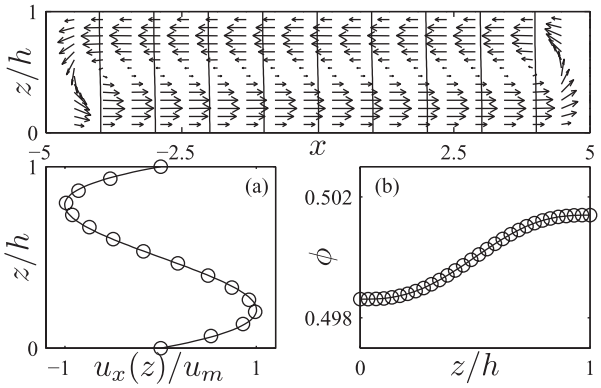

FIG. 1. Top: Steady velocity field computed from finite elements simulation of the Stokes equation and Eq. (3), in a box with aspect ratio $L = 10h$ (no-slip velocity at the boundaries and imposed ϕ at $x = \pm L/2$, $\mathrm{Ra} = 20$). Isoconcentration lines are also shown. (a) Comparison between the normalized velocity profile $u_x(z)$ at $x = 0$ computed from finite elements simulation ($\circ$, u_m is the maximal value) and the theoretical prediction, Eq. (4) (solid line). (b) ϕ at $x = 0$ vs z from the numerical simulation.

$$\nabla \cdot \boldsymbol{u} = 0, \qquad \eta \partial_z^2 u_x = \partial_x p, \qquad \partial_z p = -\rho(\phi) g, \quad (2)$$

where p is the pressure and g the gravity. The concentration ϕ follows the convection-diffusion equation:

$$\partial_t \phi + \boldsymbol{u} \cdot \nabla \phi = D \Delta \phi. \quad (3)$$

Thanks to scaling analysis [4], we can demonstrate that vertical gradients are rapidly damped by diffusion ($\partial_z \phi \approx 0$), for time scales larger than h^2/D when Ra remains moderate, i.e., $\mathrm{Ra} < \mathcal{O}(1)$. Averaging of Eq. (3) over z and assuming there is no applied pressure [4] leads to the conclusion that the transport of ϕ is mostly dominated by diffusion, i.e., $\partial_t \phi \approx D \partial_x^2 \phi$: Buoyancy-driven flows hardly affect the transport of solute in such a regime. This result comes from the fact that diffusion over z dominates convection [confined geometry and $\mathrm{Ra} < \mathcal{O}(1)$] and from the continuity equation that imposes a zero net flow rate over h, $\int_0^h dz u_x = 0$. Importantly, flow yet persists up to the relaxation of the gradients of concentration along x through diffusion. For an uniform gradient $\partial_x \phi$, this flow is given by [4]

$$u_x = \frac{\rho' g h^3 \partial_x \phi}{12 \eta} \tilde{z}(1 - \tilde{z})(2\tilde{z} - 1), \qquad u_z = 0, \quad (4)$$

where $\tilde{z} = z/h$. u_x reaches maximal values of $u_x \approx 0.008(D/h)\mathrm{Ra}$ at $\tilde{z} \approx 0.2$ and 0.8. Similar flows are also found in the problem of heat transfer across double windows [5] or in thermocapillary convection in a horizontal liquid layer [6]. Figure 1 displays numerical results from finite elements of the Stokes equation and of Eq. (3) for $\mathrm{Ra} = 20$, without the lubrication approximation ($L = 10h$) and with imposed concentrations at $x = \pm L/2$ (no-slip boundary conditions at the walls). This flow is well approximated by Eq. (4) far from the lateral walls and does not influence the concentration gradients that generate it [e.g., Fig. 1(b)] as expected, since Ra remains of the order of $\mathcal{O}(1)$ (note the prefactor 0.008 leading to $u_x h/D \approx 0.008\mathrm{Ra}$). We now illustrate such a theoretical scenario, by using several experiments that generate weak solutal gradients in confined geometries.

Confined drying.—A droplet of an aqueous solution squashed between two circular plates is left to evaporate at room temperature (Fig. 2) [7]. This confined two-dimensional geometry allows a neat control of the vapor removal from the droplet interface by diffusion and, thus, casts a typical time scale for evaporation given by $\tau_d = R_w^2/\tilde{D}$. $\tilde{D}$ depends on the diffusion coefficient of water in the vapor phase and on the volume of water molecules at saturation ($\tilde{D} \approx 2.2 \times 10^{-9}$ m^2/s at room temperature) [7]. During the receding of the air-water interface, and thus the decrease of the droplet area $\pi R_i(t)^2$, nonvolatile solutes concentrate within the droplet. Figure 2(b) shows snapshots of the drying of an aqueous colloidal dispersion: Strong concentration gradients of colloids develop close to the receding interface, eventually forming a *crust*. When

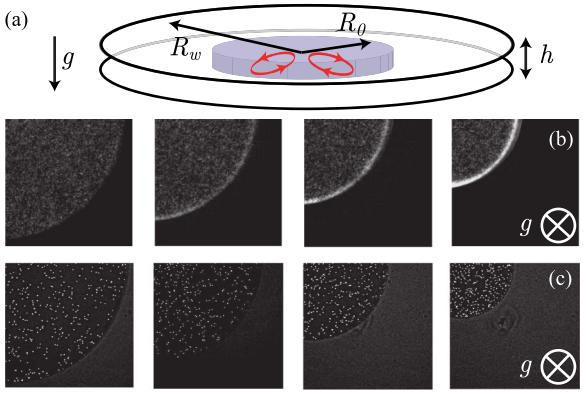

FIG. 2 (color online). (a) Evaporation of an aqueous solution from a confined droplet ($h \approx 100$–500 μm, $R_w = 4$ cm, and initial radii $R_0 = 1$–3 mm). For a binary mixture, evaporation yields concentration gradients along the radial direction that generate an axis-symmetrical buoyancy-induced flow (red loops). (b) Aqueous colloidal dispersion ($h = 140$ μm and fluorescent colloids of radius 500 nm): Concentration gradients form close to the droplet meniscus during the decrease of the droplet area. (c) The same colloids but dispersed in a water-glycerol mixture: Buoyancy-driven flows prevent the colloids from accumulating at the receding contact line [8].

the initial solution is a molecular binary mixture [e.g., water-glycerol; Fig. 2(c)] containing dispersed colloids, an axis-symmetrical flow is evidenced and convects the colloids, preventing them from accumulating at the meniscus [8]. Such a behavior has been evidenced for a wide range of binary mixtures (polymers, etc.), and the flow is always ($\rho' > 0$) directed towards $r = 0$ for $z < h/2$ and towards the interface for $z > h/2$. To definitely claim that this is an example of natural convection coming from the concentration gradients that develop within the binary mixture during evaporation, we present below a detailed model and make direct comparisons with experimental data [4].

We recently described theoretically the drying of binary mixtures (dilute up to a concentrated dispersion or solution) in such confined droplets [9]. We showed that the combined measurements during drying of the droplet area $\alpha(t) = [R_i(t)/R_0]^2$, and of the solute concentration profiles $\phi(r, t)$, can lead to estimates of thermodynamic and kinetic data of the mixture. The expected behaviors strongly depend on the Péclet number $\mathrm{Pe} = R_0^2/(D\tau_d)$ that compares solute diffusion and drying kinetics. For large Pe, significant concentration gradients develop close to the receding meniscus [Fig. 2(b) for a dilute colloidal dispersion], and the evolution of $\alpha(t)$ depends on the collective diffusion coefficient of the mixture [9].

For a small Péclet number, as is often the case for molecular binary mixtures ($D \approx 10^{-9}$ m^2/s) and using small droplets, concentration is almost homogenous over the droplet during drying $\phi(t) \approx \phi_0/\alpha(t)$, ϕ_0 being the initial concentration of the mixture. In this regime, we can

demonstrate that the concentration gradients inside the droplet are well approximated by [4]

$$\partial_r \phi(r,t) \approx \frac{\phi_0}{\alpha}\frac{2r}{R_i^2}\epsilon, \qquad \epsilon = -\frac{[a(\phi)-a_e]\tilde{D}}{4D\log(\beta\alpha)} \ll 1, \quad (5)$$

where $a(\phi) - a_e$ is the driving force of evaporation [a_e the external humidity and $a(\phi)$ the activity of the mixture] and $\beta = (R_0/R_w)^2$.

The small concentration difference across the droplet is given by $\delta\phi = \epsilon\phi_0/\alpha$ and leads to a buoyancy-driven flow $u_r(z)$ whose magnitude is estimated thanks to $\mathrm{Ra} = \rho' g h^4 \delta\phi/(\eta D R_i)$. In the framework of the lubrication approximation (confined droplet), $u_r(z)$ follows exactly Eq. (4) with gradients calculated by using Eq. (5) [4].

To test this model, we performed several experiments on glycerol-water mixtures ($\alpha = 0.2$–1, $h = 140$–450 μm, $\phi_0 = 1$–8%, $R_0 = 1.5$–2.6 mm). In this experimental range, the viscosity $\eta \approx 1$ mPa s and the interdiffusion coefficient $D \approx 10^{-9}$ m^2/s are roughly constants, $a(\phi) \approx 1$, and almost homogeneous drying always occurs [4]. We first measure velocity profiles $u_r(z)$ by using particle tracking velocimetry and a high numerical aperture objective mounted on a piezotransducer, on dilute colloidal tracers. $u_r(z)$ normalized by their maximal velocities u_m are shown Fig. 3(a) for several experiments: All the data collapse onto the z dependence given by Eq. (4). To go a step further, we performed systematic measurements of u_m at $r = R_i(t)/2$ for all the experimental range investigated. These data are shown Fig. 3(b) against Ra/h, and with the theoretical prediction given by Eqs. (4) and (5), leading to $u_r(R_i/2) \approx 0.008(D/h)\mathrm{Ra}$ with no adjustable parameters (we only use literature values for η, D, $\tilde{D}$, and ρ') [4]. The adequation with the model demonstrates without any ambiguity the origin of these hydrodynamic recirculations. Importantly, the concentration gradients leading to convection are always very small ($\delta\phi < 0.5\%$ in the experiments investigated), and the associated Ra remains small in such confined geometry. The buoyancy-driven flow [see Fig. 2(c)] therefore *does not homogenize* the binary mixture but homogenizes *only* the colloids. We

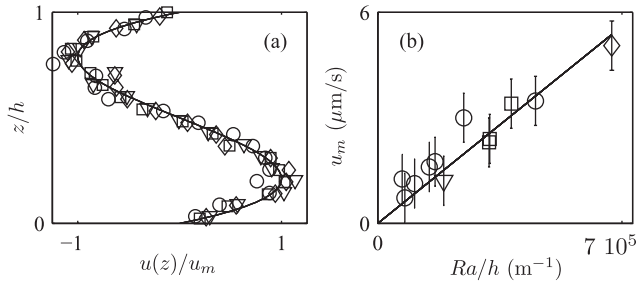

FIG. 3. (a) Normalized velocity profiles $u_r(z)$ against z/h (u_m is the maximal velocity). The continuous line is given by Eq. (4), and the symbols indicate different experimental conditions. (b) Maximal velocity u_m measured at $r = R_i/2$ against Ra/h. The continuous line is the theoretical estimation.

now illustrate briefly, thanks to two different experimental situations, the universality of such flows and their significance for the transport of colloidal species in confined geometries.

Microfluidic evaporation.—We consider pervaporation-based microfluidic devices, called *microevaporators* [10]. These tools concentrate in a controlled way solutes in aqueous solutions (from molecules to colloids), thus allowing kinetic explorations of phase diagrams. Briefly, water pervaporates through a thin poly(dimethylsiloxane) (PDMS) membrane from a nanoliter microfluidic channel, thus yielding a compensating flow from the reservoir that convects and concentrates solutes at the tip of the microchannel (Fig. 4). The detailed mechanisms at work have been investigated in depth [11]: We only evidence here regimes where sustained buoyancy-driven flows are generated [4].

For dilute mixtures, the evaporation-driven flow (averaged over the height h) is linear in the permeation zone: $v(x) = -v_0 x/L_0$, where v_0 is the mean velocity at the entrance of the microevaporator (≈ 0.1–10 μm/s) [10]. This flow convects solutes, which are accumulated in a box of size $p = \sqrt{DL_0/v_0}$, coming from the competition between convection and solute diffusion [10]. Interestingly, the chemical composition of the reservoir can be changed in time, opening the way to reach steady *out-of-equilibrium* states [11]. Solute is first accumulated during a given time, and then pure water is placed in the reservoir. After a transient, a steady concentration profile in solute is reached, from pure water up to a given concentration in solute at $x = 0$, and its shape depends on the balance between the pervaporation-driven flow and solute diffusion [4,11]. Such a *steady* gradient leads to a *permanent* buoyancy-driven flow as the density evolves along x. Because of the linearity of the Stokes equation, this natural convection (whose magnitude is given by Ra)

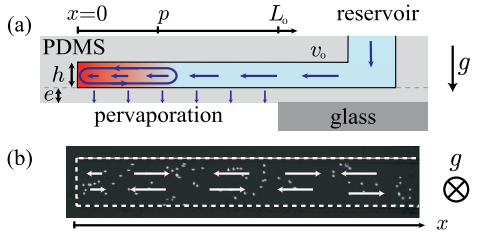

FIG. 4 (color online). (a) Sketch of a microevaporator. Permeation across the PDMS membrane of thickness e induces a flow from the reservoir that convects the solute in the microevaporator (colors mimic the concentration gradients). This gradient yields a buoyancy-induced flow (blue loop) that is superimposed to the permeation-driven flow. (b) Tip of a microevaporator: A steady concentration gradient in a water-glycerol mixture is established and induces natural convection. Fluorescent tracers (radius 500 nm) do not accumulate but follow a permanent recirculation along x (channel width 250 μm) [8].

is superimposed to the permeation-driven flow. Again, buoyancy has no influence on the gradient for moderate Ra in this confined geometry [4].

To evidence such flows and their significance on the transport of colloids, we estimate numerically thanks to Eqs. (4) and (5), the parameters (Ra, L_0, and v_0) leading to significant permanent flows on water-glycerol mixtures [4]. Then, we engineer the corresponding microevaporator ($L_0 = 7$ mm, $h = 110$ μm, width 250 μm, and $v_0 \approx 0.6$ μm/s), and we build a steady concentration profile of glycerol along x, from pure water up to $\phi \approx 20\%$ along the size $p \approx 3.4$ mm in the permeation zone [4]. This steady gradient generates a buoyancy-driven flow which is easily evidenced when fluorescent tracers are added in the reservoir [Fig. 4(b)] [8]. Colloids are first convected up to the accumulation box ($x \in [0 - p]$) and then follow a permanent loop due to buoyancy: They are not accumulated at the tip of the microevaporator, as expected when dispersed in pure water. Importantly, this experiment leads to a permanent recirculating flow for large solutes in a nanoliter chamber. The velocity of such flows, and the transit time along the loop, can be precisely controlled thanks to operational parameters (L_0, v_0, Ra, and external humidity). Such devices may thus be interesting for original biological assays. We can imagine, for instance, investigating the response of cells in such a flow to a cyclic osmotic stress driven by the concentration of the binary mixture.

Interdiffusion in a microfluidic flow.—To further demonstrate the relevance of such unavoidable solutal convection in confined geometries, we briefly consider the transverse transport of solutes between coflowing miscible liquids in a microchannel. Figure 5 displays a microfluidic cross-junction where an aqueous dispersion of colloids (radius 500 nm) flowing at a rate of 25 μL/h is focused by two streams of water (250 μL/h). The mean velocity in the downstream channel is about 1.4 mm/s (width $\times$ height 500×110 μm^2). Because of the very small diffusivity of the tracers, we do not observe any significant transverse transport (up to 1 cm downstream). This behavior considerably differs with the case depicted in Fig. 5(b), for the same conditions but with colloids dispersed in a dilute water-glycerol mixture ($\phi = 3.75\%$). The transport of the colloids is now strongly enhanced by buoyancy-driven flows induced by transverse gradients within the binary mixture. Such a result is reminiscent of recent works by Abécassis *et al.* demonstrating that gradients of salts in a similar geometry can *boost* the migration of colloids, due to diffusiophoresis [12]. Yet the migration of the colloids due to the buoyancy-driven flow is not homogeneous over the height of the channel. The regime investigated here also slightly differs from the conditions for confined drying and microevaporation. Indeed, transverse gradients in the binary mixture may be initially large, and the times scales investigated are of the order of the diffusion time over the height of the microchannel. We cannot thus exclude that a slight reorientation of the interface between the coflowing streams occurs at an early stage, as observed for regimes where mixing by diffusion is negligible [13,14]. A detailed investigation is needed to fully characterize the coupling between diffusive mixing in the binary mixture and buoyancy-driven transport of colloids. Theoretical approaches, as developed in Ref. [15] for molecular diffusivity measurements in liquid metals, may also be relevant to model such experiments. Nevertheless, these preliminary results demonstrate the very relevance of such flows for the transport of colloidal species in flowing binary mixtures.

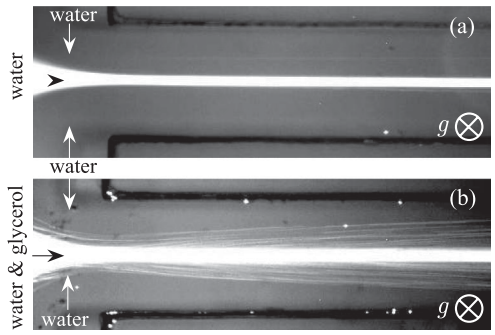

FIG. 5. (a) Pure water and dilute aqueous dispersion of fluorescent colloids flowing in a microfluidic *cross-junction* (channel width 500 μm). (b) The same conditions as above, except that the dispersion also contains glycerol: Buoyancy-driven flows efficiently disperse the colloids (long exposure time images).

Conclusions.—Solutal gradients orthogonal to the gravity lead to buoyancy-driven flows. In a confined geometry, and for moderate Ra, these flows are often neglected, as they do not influence the solutal gradients that generate them. Yet, such flows still exist and can transport efficiently larger solutes that do not diffuse efficiently. Such nontrivial effects may have a significant impact for different processes that generate concentration gradients: evaporation of droplets [16], coatings [17], chemical reactions and biological assays using coflowing microfluidic streams [2], convection of impurities during microfluidic crystallization [18,19], etc.

We thank B. Guerrier, F. Doumenc, J. Leng, and H. Bodiguel for useful discussions and Région Aquitaine, Université Bordeaux-1, Rhodia, and CNRS for funding.

[1] *Natural Convection: Heat and Mass Transfer*, edited by Y. Jaluria (Pergamon, New York, 1980).
[2] T. M. Squires and S. R. Quake, Rev. Mod. Phys. **77**, 977 (2005).
[3] H. Brenner, Physica (Amsterdam) **349A**, 60 (2005).
[4] See Supplemental Material at http://link.aps.org/supplemental/10.1103/PhysRevLett.108.198303 for details.
[5] G. K. Batchelor, Q. Appl. Math. **12**, 209 (1954).
[6] R. V. Birikh, J. Appl. Mech. Tech. Phys. **3**, 69 (1966).

[7] F. Clément and J. Leng, Langmuir **20**, 6538 (2004).
[8] See Supplemental Material at http://link.aps.org/supplemental/10.1103/PhysRevLett.108.198303 for movies.
[9] L. Daubersies and J.-B. Salmon, Phys. Rev. E **84**, 031406 (2011).
[10] J. Leng, B. Lonetti, P. Tabeling, M. Joanicot, and A. Ajdari, Phys. Rev. Lett. **96**, 084503 (2006).
[11] M. Schindler and A. Ajdari, Eur. Phys. J. E **28**, 27 (2009).
[12] B. Abécassis, C. Cottin-Bizonne, C. Ybert, A. Ajdari, and L. Bocquet, Nature Mater. **7**, 785 (2008).
[13] Y. Yamaguchi, T. Honda, M. P. Briones, K. Yamashita, M. Miyazaki, H. Nakamura, and H. Maeda, Meas. Sci. Technol. **17**, 3162 (2006).
[14] S. K. Yoon, M. Mitchell, E. R. Choban, and P. J. A. Kenis, Lab Chip **5**, 1259 (2005).
[15] D. J. Maclean and T. Alboussiere, Int. J. Heat Mass Transfer **44**, 1639 (2001).
[16] R. D. Deegan, M. Balkanski, T. F. Dupont, G. Huber, S. R. Nagel, and T. Witten, Nature (London) **389**, 827 (1997).
[17] G. Jing, H. Bodiguel, F. Doumenc, E. Sultan, and B. Guerrier, Langmuir **26**, 2288 (2010).
[18] C. Hansen and S. R. Quake, Curr. Opin. Struct. Biol. **13**, 538 (2003).
[19] R. Savino and R. Monti, J. Cryst. Growth **165**, 308 (1996).